atmosphere

MDPI

Article

Individual and Coupled Effects of Future Climate and Land Use Scenarios on Water Balance Components in an Australian Catchment

Hong Zhang [1], Bin Wang [2], Deli Liu [2,3,*], Lance M. Leslie [4], Lijie Shi [5], Mingxi Zhang [6] and Qiang Yu [7,*]

[1] School of Life Sciences, Faculty of Science, University of Technology Sydney, Broadway, Sydney, NSW 2007, Australia
[2] NSW Department of Primary Industries, Wagga Wagga Agricultural Institute, Wagga Wagga, NSW 2650, Australia
[3] Climate Change Research Centre of Excellence for Climate Extremes, University of New South Wales, Sydney, NSW 2052, Australia
[4] School of Mathematical and Physical Sciences, University of Technology Sydney, Broadway, Sydney, NSW 2007, Australia
[5] College of Hydraulic Science and Engineering, Yangzhou University, Yangzhou 225009, China
[6] Soil and Landscape Science, School of Molecular and Life Sciences, Curtin University, Perth, WA 6845, Australia
[7] State Key Laboratory of Soil Erosion and Dryland Farming on the Loess Plateau, Northwest A&F University, Xianyang 712100, China
* Correspondence: de.li.liu@dpi.nsw.gov.au (D.L.); yuq@nwafu.edu.cn (Q.Y.)

Abstract: Assessing the impacts of both climate and land use changes on hydrologic variables is crucial for sustainable development of water resources and natural ecosystems. We conducted a case study of a catchment in southwestern Australia to assess the impacts of future climate and land use changes, both separately and in combination, on water resource availability. For this evaluation, the Soil and Water Assessment Tool (SWAT) model was first calibrated and then forced by 34 global climate models (GCMs), under two Representative Concentration Pathways (RCP4.5 and RCP8.5) and five land use scenarios (LU0–4). Our results suggested that SWAT reproduced the observed monthly streamflow well. Land use changes have impacts on all hydrologic variables, especially on runoff at the annual scale. Future runoff was projected to decrease in all seasons, especially winter and spring. For the combined effects of climate and land use changes, the results of LU1–4 were only slightly different from the response of LU0. An uncertainty analysis shows that GCMs had the greatest contribution to hydrologic variables, followed by RCPs and land use scenarios. Hence, it is advisable for impacts analysis to use an ensemble of GCMs under different RCPs to minimize the uncertainty of projected future hydrologic variables.

Keywords: climate change; land use change; GCM; southwestern Australia; runoff

Citation: Zhang, H.; Wang, B.; Liu, D.; Leslie, L.M.; Shi, L.; Zhang, M.; Yu, Q. Individual and Coupled Effects of Future Climate and Land Use Scenarios on Water Balance Components in an Australian Catchment. *Atmosphere* **2022**, *13*, 1428. https://doi.org/10.3390/atmos13091428

Academic Editor: Gianni Bellocchi

Received: 19 July 2022
Accepted: 31 August 2022
Published: 3 September 2022

1. Introduction

Global warming is likely to accelerate hydrologic cycle through increasing atmospheric evaporative demand and changing the intensity, frequency and duration of rainfall events [1,2]. Hydrologic variables (e.g., runoff, evapotranspiration, and soil water) are highly sensitive to even small changes in rainfall and temperature [2–4]. Thus, hydrologic sensitivity to climate change has been widely discussed [5], due to the importance of water availability for human society and ecosystem processes [4], and for the development of appropriate water resources management strategies [6]. For instance, the regression between global temperature and runoff shows that a 1 °C rise in temperature is associated with a 4% rise in runoff [7]. However, Legates, Lins [8] argued that this conclusion was

not supported by the data presented by Labat, Goddéris [7]. In addition, such global trends should be studied on a regional scale where there are both increasing and decreasing trends. Basin level hydrologic analyses, therefore, are needed to assess the sensitivity of the basin to climate change scenarios.

In addition to climate change, the hydrologic cycle is also influenced by land use change, resulting from human activities such as replacing natural forests and wetlands with croplands and built-up land [9]. According to a recent IPCC report [10], about 25% of the ice-free land on Earth is being degraded by human activities (medium confidence, which reflects medium evidence and agreement in the magnitude of response). Therefore, land use is a key factor in influencing the hydrologic response, primarily due to changes in vegetation cover that alter rainfall interception and infiltration, thereby changing runoff [11]. In addition to runoff, land use change has been considered as a driver to nearly all hydrologic processes such as evapotranspiration [12,13] and soil water [14]. The impacts of land use change on hydrology have been studied and debated for many years throughout the world [15,16]. In hydrologic responses to land use change studies, hydrologic effects of forest have attracted much attention, especially deforestation and afforestation impacts. Several studies reported that forest changes greatly affect water yield, although the magnitude of change varies greatly between catchments (e.g., semi-arid Loess Plateau region and tropical forest area [17,18]). In contrast, limited effects (e.g., the Canadian boreal forest area) [19], no effects (e.g., the Duero river basin) [20], or even positive effects (e.g., Guangdong Province, China) [21] on water yield due to forest changes have been found in other studies, especially in large basins [22]. Therefore, a detailed investigation of land use change effects on the hydrologic cycle of a specific catchment is highly valuable for developing catchment management policies.

Since 1910, the mean near-surface temperature in Australia has risen by ~0.9 °C, with the nighttime minimum rising more than the daytime maximum [23]. In addition to climate warming, southwestern Australia (SWA) has experienced a substantial decrease in rainfall over the last century [24], and the climate impacts on its water resources have been particularly acute [25]. For instance, rainfall has decreased by 16% since the mid-1970s, resulting in a reduction of more than 50% of stream flows into the main reservoirs in the area, which provides water for the state capital (Perth) [26]. The water shortage is expected to worsen, as climate change projections suggest that rainfall will decrease further over SWA in the future [27,28] and the percentage changes in rainfall will be amplified in decreased runoff [29]. In addition, up to 20% more droughts are projected by 2030 in most parts of Australia and up to 80% more droughts by 2070 in SWA [30]. Furthermore, catchments in SWA have been subjected to extensive land clearing [31], so because of the importance of forests in Earth-–atmosphere interactions, the ability to project the possible impacts of land use change on hydrology is seen as a key management tool [32]. While some studies have assessed the hydrologic response to climate change in SWA [33,34], there have been few detailed studies of the coupling impacts of coincident climate and land use changes on individual catchments in SWA [35]. These coupling effects of climate and land use changes on regional runoff regimes are complex and as yet poorly understood. Consequently, a catchment representative of SWA was examined in this study to provide detailed insights that suggest future options for water management under concurrent climate and land use changes.

The climate change impacts studies are generally related to uncertainties that are stemmed from each step of the entire hydroclimatic modeling chain, i.e., uncertainty in Global Climate Models (GCMs) projections, downscaling methods uncertainty, and modeled hydrologic regimes uncertainty [2]. The uncertainty resulting from hydrologic simulations was quite small when compared to the climate model according to comparison studies [2,36]. This might be due to the fact that the hydrologic cycle is sensitive to changes in precipitation [37] and GCMs project large variations in rainfall change [4]. Due to the considerable uncertainty in GCM predictions, the outputs of multiple GCMs are typically used to evaluate the hydrologic response to climate change [38,39].

Both climate and land use changes have strong impacts on water resources. The combined effects of climate and land use changes are not simply the sum of the two effects [40]. Therefore, the study of climate change and land use change impacts on hydrology within a catchment has become a major research topic [41]. Currently, hydrologic modeling is the most widely used method to quantify and evaluate the impacts of climate change and land use change on the water cycle [42]. The Soil and Water Assessment Tool (SWAT) is a physically based and semi-distributed watershed hydrologic model developed by Arnold, Srinivasan [43]. It can simulate long-term hydrologic variables, such as streamflow, on daily or monthly time scales [44], under different climatic and land-use conditions. The SWAT model has been demonstrated to be effective for quantifying the hydrologic response to environmental changes [45]. In recent years, there have been some studies using SWAT for assessment of the hydrologic response to future climate and land use changes [46–48], including a few catchments in Australia [49]. However, to the best of our knowledge, there are very few studies using the SWAT model for hydrologic response analysis under multiple GCMs and land use change scenarios for southwestern Australia. Consequently, this study is the first to use the SWAT model, run with statistically downscaled daily climate data from 34 GCMs and 4 land use change scenarios, to assess the hydrologic response to a combination of climate change and land use change of a principal catchment in SWA.

Specifically, our aim was to evaluate the impacts of climate change and land use change on hydrology in Wooroloo Brook catchment, SWA, as a case study. Hence, the components of this study were to: (1) evaluate the performance of the SWAT model in this catchment and assess the impacts of future climate and land use changes, both separately and in combination, on hydrologic variables (runoff, actual evapotranspiration, and soil water); and (2) quantify the contribution of GCM, RCP, and land use scenarios to the overall uncertainty in future changes of hydrologic variables.

2. Materials and Methods

2.1. Study Area

The Swan-Avon River catchment is located in SWA, covering an area of more than 120,000 km^2, including parts of Perth's metropolitan area [50]. About 65% of the Avon River basin has been cleared of its native woodland vegetation for cereal production and sheep grazing, resulting in substantially increased soil erosion [51]. The Swan Coastal Plain has also been extensively cleared for agriculture and urban development [52,53]. Wooroloo Brook is one of the major tributaries of the Swan River in the Swan Coastal basin [54]. The Wooroloo Brook catchment above Karls Ranch (Figure 1) was chosen as the case study region. This catchment is around 511 km^2 with elevation between 84 and 448 m. According to statistics in 1977–2016, the mean annual temperature was about 17.4 °C, mean annual rainfall was around 737.5 mm, and mean annual runoff was approximately 75.5 mm in this catchment. There has been a significant decreasing trend ("*p* value" ≤ 0.01) in annual runoff resulting from decreasing rainfall in the Wooroloo Brook catchment above Karls Ranch in recent decades according to the Mann–Kendall trend test. However, very few studies have been conducted regarding the hydrologic response to climate change in the Wooroloo Brook catchment. Consequently, this study is a step towards assessing the combined effects of climate and land use changes on catchment hydrology and can help inform and support regional priorities for future water management, with respect to both climate and land use changes in SWA.

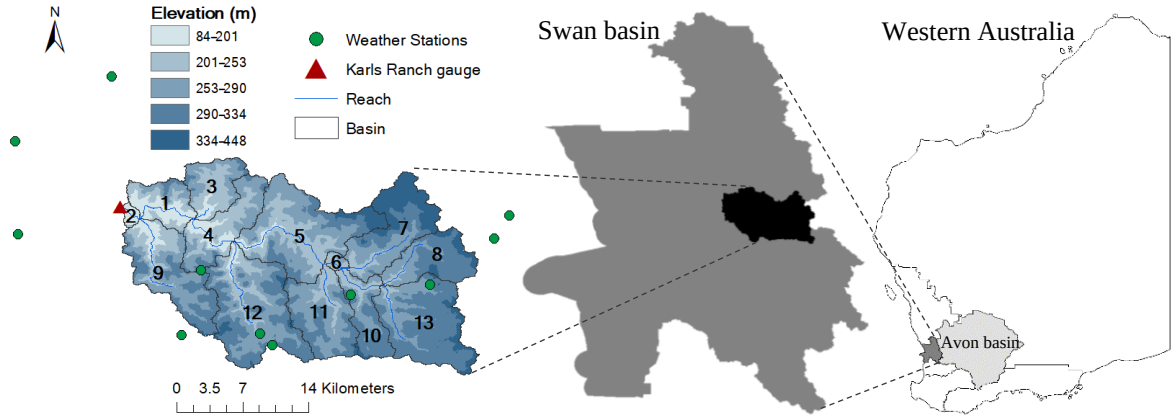

Figure 1. Location map of the Wooroloo Brook catchment (consists of 13 sub–basins).

2.2. The SWAT Model

The SWAT model [43] is a physically based and long-term simulation watershed model, which runs on a daily time step. It has proved to be an effective means for assessment of water resources over a broad range of scales, globally [55]. A modified Soil Conservation Service Curve Number (SCS CN) approach [56] was used in SWAT to calculate runoff. Using the SCS CN method, SWAT allows the users to evaluate the relative impacts of climate and land cover changes at the sub-basin level [57]. SWAT has been used successfully to model environmental change impacts on hydrology, making it a widely used hydrologic tool in land use change and climate change studies [57–59]. However, there are limited examples from western Australia, with most research having focused on the far more populous eastern and southeastern Australia [60]. Hence, this study applied the SWAT model to examine the impacts of climate and land use changes on hydrology for a catchment in SWA. The Hargreaves method, using air temperature as input data, was selected to simulate the potential evapotranspiration in the SWAT model [6,61]. For further model details, see Arnold, Srinivasan [43].

2.3. Data Preparation

For development of a semi-distributed hydrologic model, various data series are needed as inputs to the SWAT model. Processing of the specific data is described in this section, and the input data for the SWAT model, sources of the data, and related characteristics of the data are shown in Table 1.

Table 1. Data input for the SWAT model, data sources, and related characteristics.

Data	Source	Related Characteristics
DEM (Digital elevation model)	Geoscience Australia	1 s resolution SRTM (Shuttle Rader Topography Mission) derived DEM
Land use/land cover map	Australian Bureau of Agricultural and Resource Economics and Sciences (ABARES)	50 m spatial resolution
Soil map	Bureau of rural sciences, Australia	Published at a scale of 1:2,000,000
Observed streamflow	Bureau of Meteorology (BOM)	Mean daily streamflow (1977–2007, 2009–2017)
Observed climate data	BOM	Maximum and minimum daily temperature and rainfall (1974–2017)
Climate data based on 34 GCMs under RCP4.5 and RCP8.5 scenarios	Office of Science, US Department of Energy, downscaled by Liu and Zuo [62]	Maximum and minimum daily temperature and rainfall (1900–2100)

2.3.1. DEM, Land Use, and Soil

DEM, land use, soil, and slope characteristics are basic inputs for the HRU (hydrologic response unit) definition in the SWAT model [63]. The details of the data sources adopted in this research are introduced below.

DEM is required by the SWAT model for delineating watershed and generating sub-basins in the Wooroloo Brook catchment (Figure 1). In this study, the DEM data were downloaded from Geoscience Australia (https://elevation.fsdf.org.au/, accessed on 10 July 2019) with a resolution of 30 m by 30 m, and 13 sub-basins were generated (Figure 1). Sub-basin parameters (e.g., slope gradient and channel length) were obtained from DEM.

Land use is one of the key factors that impacts evapotranspiration and runoff in a basin [64]. Land use data with a 50 m spatial resolution from ABARES was adopted and reclassified to match the land use classes in the SWAT model (Figure 2) in this study. This data was obtained through the integration of fine-scale satellite data, land tenure, and other kinds of land use information, and information gathered in the field. There were three land use classes in the study area: FRST (forest-mixed), RNGE (range-grasses), and URBN (urban) (Figure 2).

The SWAT model needs a soil map and a soil database, which contains multiple soil characteristics such as the depth of the soil surface to the layer bottom, soil bulk density, and saturated hydraulic conductivity for different soil layers [65]. The soil map was taken from the Digital Atlas of Australian Soil for the Wooroloo Brook catchment (Figure 2), and a "usersoil" database was created according to lookup tables and previous research [65,66].

After DEM, land use, and soil input in the ArcSWAT interface, this study defined 5 slope classes (0–10%, 10–20%, 20–30%, 30–50%, and >50%) for slope discretization. Finally, thresholds of 0%–0%–0% were defined for land use, soil, and slope using a multiple HRU generation approach and 268 HRUs were produced using the ArcSWAT interface.

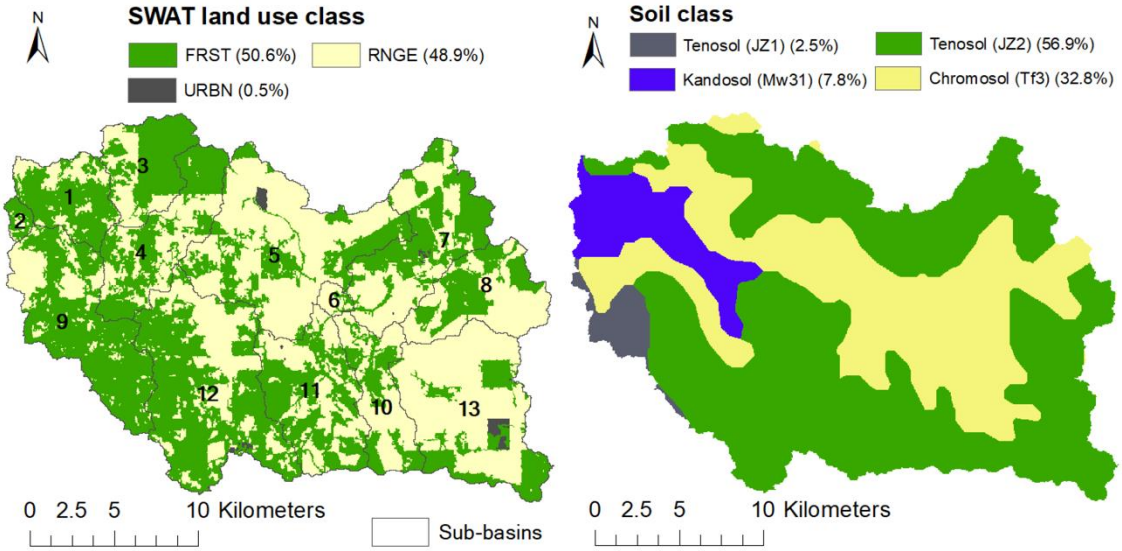

Figure 2. The maps of land use classification (**left**) and soil (**right**) in the SWAT model for the Wooroloo Brook catchment (consists of 13 sub–basins), SWA.

2.3.2. Climate Data and Streamflow

Daily rainfall and maximum and minimum temperature at 11 weather stations in 1974–2017, used for driving SWAT model simulations, were collected from the Bureau of Meteorology (BOM) (http://www.bom.gov.au/climate/data/, accessed on 7 May 2018). Based on the default settings of SWAT, each sub-basin was assigned a climate station that was nearest to the centroid of the sub-basin [67]. For the calibration and validation of streamflow, daily observed streamflow at the outlet (Karls Ranch gauge) of the catchment

was obtained from the BOM (http://www.bom.gov.au/waterdata/, accessed on 7 May 2018). To set model parameters for a great variety of climatic conditions, a period for streamflow calibration, including dry, normal, and wet years, was chosen in this study. Therefore, the periods of 1992–2017 (1989–1991 as warm-up, streamflow for 2008 was missing) and 1977–1991 (1974–1976 as warm-up) were selected for streamflow calibration and validation, respectively. Therefore, the periods of 1992–2017 (1989–1991 as warm-up) and 1977–1991 (1974–1976 as warm-up) were selected for streamflow calibration and validation at a monthly time scale, respectively. The observed streamflow data for 2008 was missing.

2.4. Calibration and Evaluation Methods for the SWAT Model

Calibration and Uncertainty Programs (SWAT-CUP) has become a widely used computer program developed for calibration, validation, and uncertainty analysis of SWAT [68,69]. The program Sequential Uncertainty Fitting Ver. 2 (SUFI-2) [70] in SWAT-CUP was chosen for the SWAT model parameters' calibration, validation, and uncertainty analysis in this study. The sensitivity of 22 parameters in the SWAT model was ranked using the global sensitivity analysis approach available in SUFI-2.

In this research, the results for climatic and hydrologic variables were all shown at monthly or annual time scales, so the modeling process would be more efficient with streamflow calibrated at a monthly rather than a daily time scale. Thus, monthly simulated and observed streamflow in 1992–2017 (2008 was missing) and 1977–1991 were used for the SWAT model calibration and validation, respectively. Using the SUFI-2 procedure, 4 iterations with 1000 model runs in each iteration were run to maximize th Nash–Sutcliffe Efficiency (NSE) [71]. Percent bias (PBIAS), NSE, and coefficient of determination (R^2) were selected as statistical evaluation criteria [72] in this study and were calculated as follows:

$$PBIAS = 100\left(\frac{\sum_{i=1}^{N}(Q_{sim,i}-Q_{obs,i})}{\sum_{i=1}^{N}(Q_{obs,i})}\right) \quad (1)$$

$$NSE = 1 - \frac{\sum_{i=1}^{N}\left(Q_{obs,i}-Q_{sim,i}\right)^2}{\sum_{i=1}^{N}\left(Q_{obs,i}-\overline{Q}_{obs}\right)^2} \quad (2)$$

$$R^2 = \frac{\left[\sum_{i=1}^{N}(Q_{obs,i}-\bar{Q}_{obs})\,(Q_{sim,i}-\bar{Q}_{sim})\right]^2}{\sum_{i=1}^{N}(Q_{obs,i}-\bar{Q}_{obs})^2\sum_{i=1}^{N}(Q_{sim,i}-\bar{Q}_{sim})^2} \quad (3)$$

where i is the ith sample; N is the number of samples; Q_{sim} and Q_{obs} are simulated and observed monthly streamflow (m^3/s), respectively; $\bar{Q}_{sim}$ and $\bar{Q}_{obs}$ are the average simulated and observed monthly streamflow (m^3/s), respectively.

2.5. Statistical Downscaling Method

Using the statistical downscaling method NWAI-WG [62], gridded climate data from GCMs at a monthly time scale were downscaled to the weather stations at a daily time scale. First, an inverse distance-weighted interpolation approach was applied to downscale the monthly GCMs climate data to specific sites. A bias correction was then used to correct monthly GCM simulations for each station. Third, a stochastic weather generator was used to generate daily climatic variables for each station. More specific and detailed steps about this downscaling method can be found in [62]. The validation conducted by Liu and Zuo [62] indicated that this downscaling approach can reproduce the observed climate data at daily, monthly, and yearly time scales well. In this research, a post downscaling treatment was applied to the NWAI-WG model downscaled climate data. When applying downscaled data to a catchment, the existence of inconsistent daily rainfalls among stations could lead to: (1) more rainfall days and (2) less daily rainfall for the catchment and possibly poor modeling of high flows. Therefore, the central station of the catchment was selected as the reference station and the other 10 stations were re-

downscaled to have the matching rainfall events with the rainfall quantities for each station. This post downscaling treatment is validated according to the hypothesis that the climate stations are near enough so that the rainfall days are quite uniform. This study area is about 515 km^2; that is, the radius is around 12.8 km. Therefore, this catchment downscaling approach was considered valid for this study.

In this study, 34 GCMs [73] from the Coupled Model Inter-comparison Project 5 (CMIP5) were used to minimize the uncertainty created by the selection of GCMs. Two RCPs (representative concentration pathways) were selected to represent the likely future greenhouse gas concentrations, with RCP 4.5 and RCP 8.5 representing intermediate and high emission scenarios, respectively [49]. In this research, the period of 1977–2016 was defined as the baseline, 2021–2060 was defined as the near future, or 2040s, and 2061–2100 as the far future, or 2080s. To show the range of future climate projections, changes at seasonal and annual time scales in the maximum and minimum temperature and rainfall of 34 GCMs in 2040s and 2080s compared to the baseline period were calculated for this catchment. Furthermore, to provide the range of future hydrologic projection, changes in runoff, actual evapotranspiration (ET), and soil water (SW) at seasonal and annual time scales of 34 GCMs in the 2040s and 2080s compared to the baseline were estimated. In this study, we defined four seasons, i.e., spring (September–November), summer (December–February), autumn (March–May), and winter (June–August).

2.6. Different Land Use Change Scenarios

In this catchment, there were three land use classes (i.e., forest-mixed (50.6%), range-grasses (48.9%), and urban (0.5%)) based on SWAT land use classes reclassification. To assess the hydrologic response to land use change in the catchment, four hypothetical land use change scenarios (Table 2) were considered, based on present land use conditions and possible future land use plans. The present land use (year of 2008) (Figure 2) is hereafter mentioned as LU0 (land use 0), and the four land use change scenarios are mentioned as LU1–4 (land use 1–4). The Land Use Update tool [74] in the SWAT model was used to implement these changes at the sub-basin scale. For example, FRST is expected to be changed to URBN only when the two land use classes occur in the same sub-basin [49]. LU1 assumes that 50% (relative to FRST area) of current FRST will be converted to RNGE while the remaining land uses stay unchanged, representing a 25.3% (relative to the whole catchment area) increase in RNGE area. The details of the other land use change scenarios can be found in Table 2, and the land use proportions for LU0–4 are shown in Table S1.

Table 2. The four land use change scenarios based on LU0 (i.e., forest-mixed (50.6%), range-grasses (48.9%), and urban (0.5%)) in the Wooroloo Brook catchment, southwestern Australia.

LU1	Deforestation	Assumes that 50% of current FRST will be changed to RNGE while the remaining land uses stay unchanged, i.e., 25.3% increase of RNGE area
LU2	Urbanization/deforestation	Assumes that 100% of current FRST will be converted to URBN while the remaining land uses stay unchanged, i.e., 23.8% increase of URBN area
LU3	Afforestation	Assumes that 50% of current RNGE will be changed to FRST while the remaining land uses stay unchanged, i.e., 24.4% increase of FRST area
LU4	Urbanization	Assumes that 100% of current RNGE will be converted to URBN while the remaining land uses stay unchanged, i.e., 29.5% increase of URBN area

2.7. Contribution Analysis of Uncertainty

In uncertainty analysis, the analysis of variance (ANOVA) method has been widely adopted to estimate the contribution of various sources [75,76]. In this study, a three-way ANOVA (three factors) was used to calculate the contribution of GCM, RCP, and land use (LU) scenarios to the uncertainty in future changes of runoff, ET, and soil water. The three-way ANOVA could be divided into seven parts with three main effects and four interaction effects. Thus, the total sum of squares (SST) was quantified as:

$$SST = \underbrace{SS_{GCM} + SS_{RCP} + SS_{LU}}_{main\ effects} + \underbrace{SS_{GCM:RCP} + SS_{GCM:LU} + SS_{RCP:LU} + SS_{GCM:RCP:LU}}_{interaction\ terms} \quad (4)$$

The entire process of this study was shown in Figure 3.

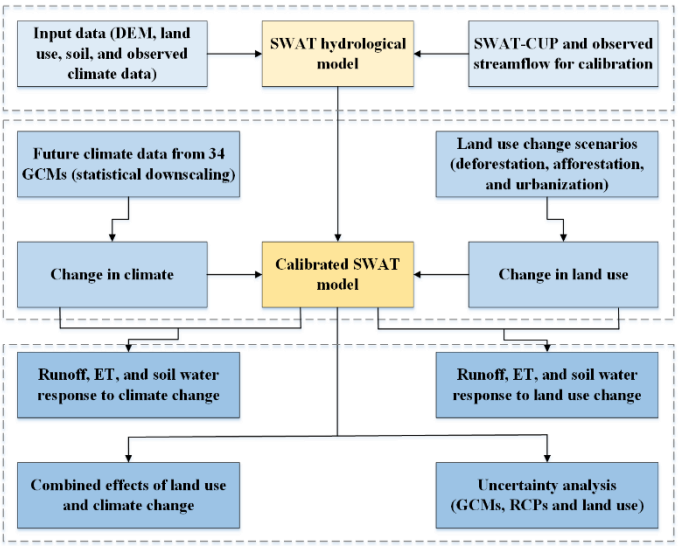

Figure 3. Flow chart of climate hydrological modeling in this study.

3. Results

3.1. Streamflow Simulation

For streamflow calibration, 22 parameters of the SWAT model were calibrated, validated, and ranked for the Wooroloo Brook catchment (Table S2). Global sensitivity analysis in SWAT-CUP was used to rank these parameters based on their sensitivities. The sensitivity analysis indicated that six parameters (ranked 1–6, Table S2) had significant impacts on the calibration of the SWAT model ($p \leq 0.05$). In this catchment, the SCS runoff curve number for moisture condition II (CN2) was found to be the most sensitive calibration parameter. The comparison between monthly simulated and observed streamflow during calibration and validation is shown in Figure S1. A visual comparison suggests that the simulations reasonably reproduced the observed streamflow and similarly replicated its temporal fluctuation. Figure 4 indicates that monthly simulated and observed runoff had a high correlation (NSE ≥ 0.86, $R^2 \geq 0.87$, and |PBIAS| ≤ 8.3%) in model calibration and validation in the Wooroloo Brook catchment.

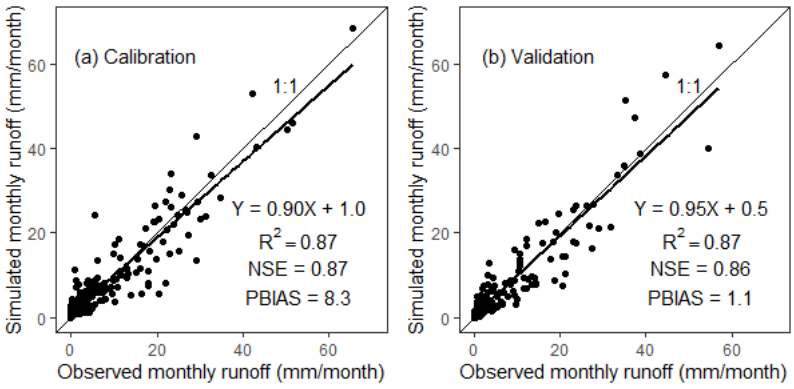

Figure 4. Correlation of monthly simulated and observed runoff in model calibration and validation in the Wooroloo Brook catchment, southwestern Australia.

3.2. Hydrologic Response to Land Use Change

Monthly runoff, actual evapotranspiration, and soil water were simulated using the calibrated SWAT under LU0–4, in 1977–2016, for the Wooroloo Brook catchment. Figure 5 displays the seasonal runoff, ET, and SW under land use 0–4 while Table 3 shows changes in the annual runoff, ET, and SW under LU0–4. There were clear seasonal variations for runoff, ET, and SW, with values greatest in winter (wet season) and least in summer (dry season) (Figure 5). Moreover, in Figure 5, seasonal changes in the runoff under LU1–4 were generally more remarkable than changes in ET and SW, especially in winter. In addition, Figure 5 suggests that seasonal runoff increased under LU1–2 and LU4 (deforestation or urbanization) while it decreased under LU3 (afforestation), and the same result for annual runoff can be found in Table 3. For example, runoff increased by 4 mm (6%) under LU1 (25.3% increase in RNGE from FRST), 17 mm (22.8%) under LU2 (23.8% increase in URBN from FRST), and 18 mm (25.1%) under LU4 (29.5% increase in URBN from RNGE) using the SWAT model. In comparison, a 24.4% increase in FRST area from RNGE (LU3) caused a −3 mm (−4.3%) decrease in runoff. In contrast to runoff, Table 3 shows that the mean annual actual evapotranspiration decreased under LU1–2 and LU4 (deforestation or urbanization) while it increased under LU3 (afforestation). In addition, the percentage changes in annual ET were much smaller than that of runoff under LU1–4 (Table 3). For instance, average annual ET decreased by −6 mm (−1.0%) with a 25.3% decline in FRST (LU1) and increased by 5 mm (0.9%) with a 24.4% increase in FRST area (LU3) using SWAT. Furthermore, mean annual soil water increased by 4.4% under LU1 (25.3% increase in RNGE from FRST) and very little (≤0.2%) under LU2 (23.8% increase in URBN from FRST) while it decreased by −4.2% under LU3 (24.4% increase in FRST from RNGE) and −4.6% under LU4 (29.5% increase in URBN from RNGE) using SWAT.

Table 3. Changes in mean annual runoff, actual evapotranspiration, and soil water using the SWAT model under LU0–4 in the Wooroloo Brook catchment, southwestern Australia in 1977–2016.

Hydrologic Variables		LU0	LU1	LU2	LU3	LU4
Runoff	Value (mm)	73	77	90	70	91
	Absolute change (mm)	0	4	17	−3	18
	Percentage change (%)	0.0	6.0	22.8	−4.3	25.1
ET	Value (mm)	568	562	558	573	561
	Absolute change (mm)	0	−6	−10	5	−7
	Percentage change (%)	0.0	−1.0	−1.8	0.9	−1.3
SW	Value (mm)	26.6	27.7	26.6	25.4	25.3
	Absolute change (mm)	0.0	1.2	0.0	−1.1	−1.2
	Percentage change (%)	0.0	4.4	0.2	−4.2	−4.6

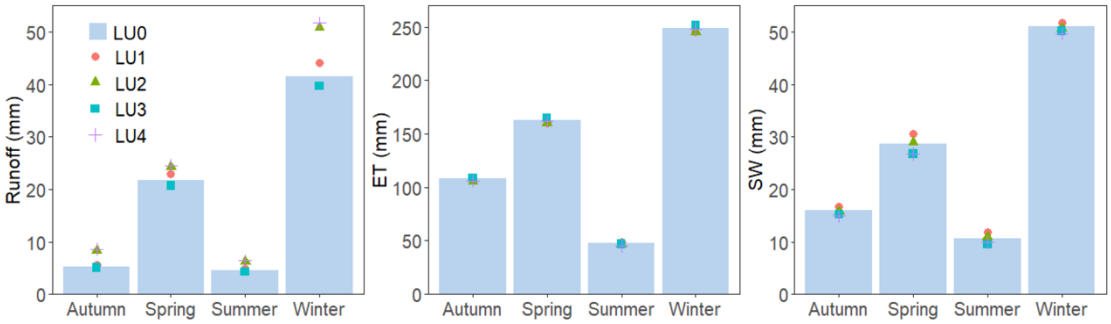

Figure 5. Seasonal runoff, ET, and SW in 1977–2016 under land use 0–4 in the Wooroloo Brook catchment, SWA.

3.3. Projected Changes in Climatic Variables

Future temperature and rainfall projections were aggregated to seasonal and annual time scales and compared to baseline values (Figure 6). In this study, all 34 GCMs were in

agreement that the temperature would rise in the future, with greater temperature increases in the 2080s than in the 2040s at both seasonal and annual time scales (Figure 6). In addition, higher temperature increases were projected under RCP8.5 than RCP4.5 (Figure 6). Figure 6a,b shows that the seasonal maximum temperature was mainly predicted to increase most in spring in the future while increases were mainly the lowest in winter. For temperature minima (Figure 6c,d), the median estimate exhibited the largest increase mainly in autumn, and the smallest increase in the minimum temperature in winter. The ensemble median increase for the annual maximum temperature was 1.1 °C in 2040s (RCP 4.5), 1.3 °C in 2040s (RCP 8.5), 1.8 °C in 2080s (RCP 4.5), and 3.4 °C in 2080s (RCP 8.5) (Figure 6a,b) while the annual minimum temperature was projected to increase by 1.0 °C in 2040s (RCP 4.5), 1.2 °C in 2040s (RCP 8.5), 1.6 °C in 2080s (RCP 4.5), and 3.2 °C in 2080s (RCP 8.5) (Figure 6c,d).

Future rainfall changes vary across seasons and across GCMs, with most GCMs projecting decreases at both seasonal and annual time scales (Figure 6e,f). Future rainfall decreased more in spring and winter while it decreased less in summer and autumn under both RCPs. The largest ensemble median decrease in rainfall occurred in spring while median summer rainfall was predicted to have the smallest future changes (Figure 6e,f). At annual time scale in 2040s, the decreases in rainfall projected by the 34 GCMs ranged from −12.4% (25th percentage) to −3.3% (75th percentage) under RCP 4.5 and −14.6% (25th percentage) to −6.9% (75th percentage) under RCP 8.5, with the ensemble median of −8.7% and −11.0%, respectively. More decreases were projected for annual rainfall in 2080s, with −11.7% (−15.3 to −7.9%) under RCP 4.5, and −22.6% (−32.9 to −16.2%) under RCP 8.5. The uncertainty range, in brackets, shows the 25th and 75th percentage of the 34 GCMs in this study.

Figure 6. Projected seasonal and annual changes in temperature (°C) and rainfall (%) in 2040s and 2080s under both RCPs based on 34 GCMs compared to the baseline period. Data displayed are changes in the 40−year averages for each of the 34 GCMs. The lower and upper whiskers show the 10th and 90th percentiles; box boundaries show the 25th and 75th percentiles; the black line within each box marks the median values.

3.4. Hydrologic Responses to Future Climate Change

Projected runoff, ET, and SW were aggregated into seasonal and annual time scales and were compared to the baseline values. Similar to rainfall, changes in future runoff differ across seasons and across GCMs, with most GCMs exhibiting decreases at both seasonal and annual time scales (Figure 7—LU0). Future runoff was projected to decrease more in winter and spring but decrease less in autumn and summer under both RCPs. Additionally, annual runoff in 2080s decreased more than those predicted in the 2040s, and annual runoff also showed more decreases under RCP8.5 than RCP4.5 (Figure 7). The largest runoff, which was in winter in baseline (Figure 5), was predicted to decrease most (−20.6% in 2040s (RCP 4.5), −41.2% in 2080s (RCP 4.5), and −62.3% in 2080s (RCP 8.5)) among the four seasons except in 2040s (RCP 8.5) when runoff decreased the most in spring (−34.0%). In addition, runoff was projected to decline least in autumn among the four seasons except in 2040s (RCP4.5) when runoff decreased the least in summer. Annual runoff changes projected by the 34 GCMs in 2040s varied from −31.6% (25th percentage) to 3.2% (75th percentage) under RCP 4.5 and −39.1% (25th percentage) to −4.1% (75th percentage) under RCP 8.5, with the median values of −19.4% and −28.3%, respectively. More decreases were projected for annual runoff in 2080s, with −33.6% (−45.0 to −14.4%) under RCP 4.5 and −55.3% (−68.1 to −41.2%) under RCP 8.5.

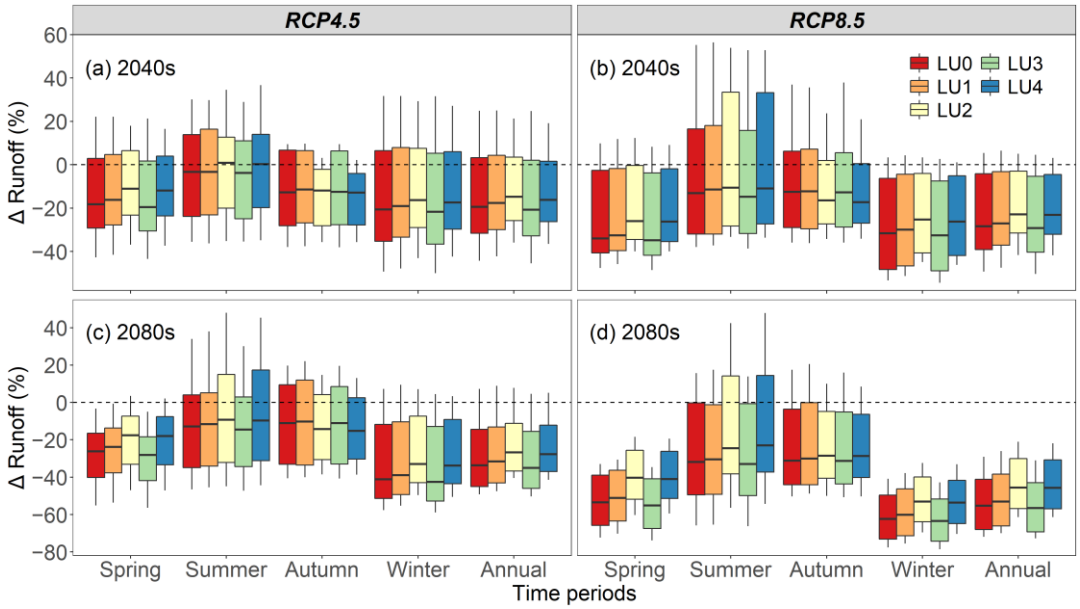

Figure 7. Projected seasonal and annual changes in runoff (%) for LU0−LU4 in the 2040s and 2080s under both RCPs estimated from 34 GCMs compared to the baseline period. Data displayed are changes in the 40−year averages for each of the 34 GCMs. The lower and upper whiskers show the 10th and 90th percentiles; box boundaries show the 25th and 75th percentiles; the black line within each box marks the median values.

For actual evapotranspiration (ET), the majority of the 34 GCMs simulated decreases at both seasonal and annual time scales except in autumn in 2040s (Figure 8—LU0). The changes in ET were smaller than the simulated changes in runoff (Figures 7 and 8). In autumn in 2040s, ET was projected to increase by 2.2% under RCP 4.5 and 3.0% under RCP 8.5 according to the ensemble median of the GCMs. At seasonal time scales (Figure 8—LU0), future ET was predicted to decrease most in spring. At the annual time scale in 2040s, changes in ET simulated by the 34 GCMs varied from −7.8% (25th percentage) to −3.5% (75th percentage) under RCP 4.5 and −10.0% (25th percentage) to −3.5% (75th percentage) under RCP 8.5, with median values of −5.1% and −6.0%, respectively (Figure 8—LU0). More decreases were projected for annual ET in 2080s, with −7.5% under RCP 4.5 and −15.8% under RCP 8.5. In addition, median estimates suggested that there was a trend

of decreasing soil water at seasonal and annual time scales in both future periods under both RCPs (Figure 9—LU0). Furthermore, the ensemble median showed decreases of −15.0% in 2040s (RCP4.5), −16.0% in 2040s (RCP8.5), −17.7% in 2080s (RCP4.5), and −30.0% in 2080s (RCP8.5).

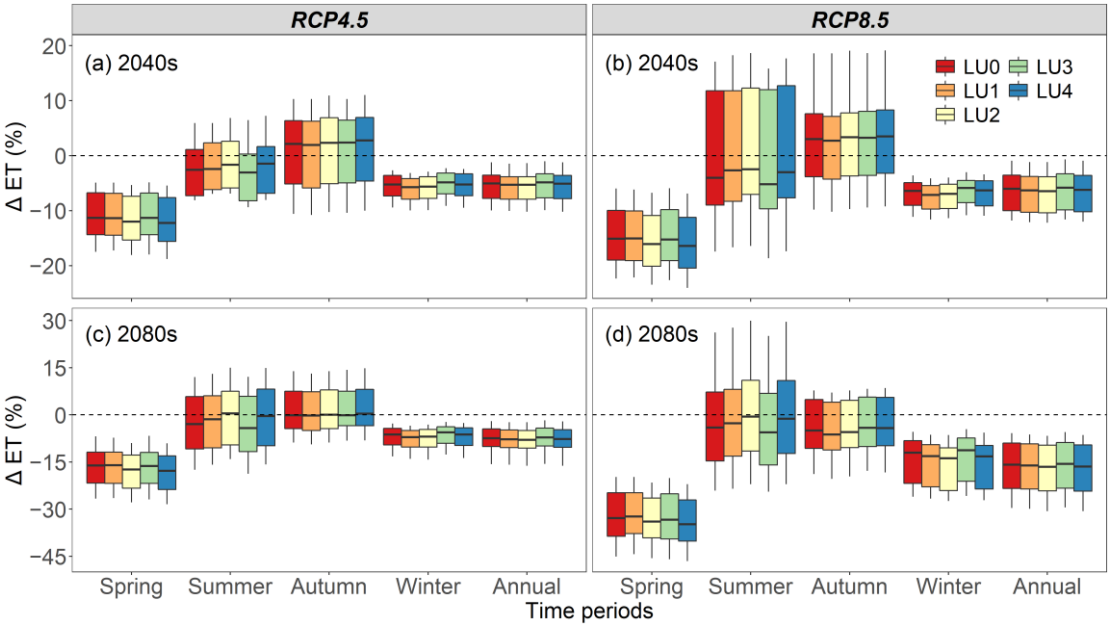

Figure 8. Projected seasonal and annual changes in ET (%) for LU0–LU4 in the 2040s and 2080s under both RCPs estimated from 34 GCMs compared to the baseline period. Data displayed are changes in the 40−year averages for each of the 34 GCMs. The lower and upper whiskers show the 10th and 90th percentiles; box boundaries show the 25th and 75th percentiles; the black line within each box marks the median values.

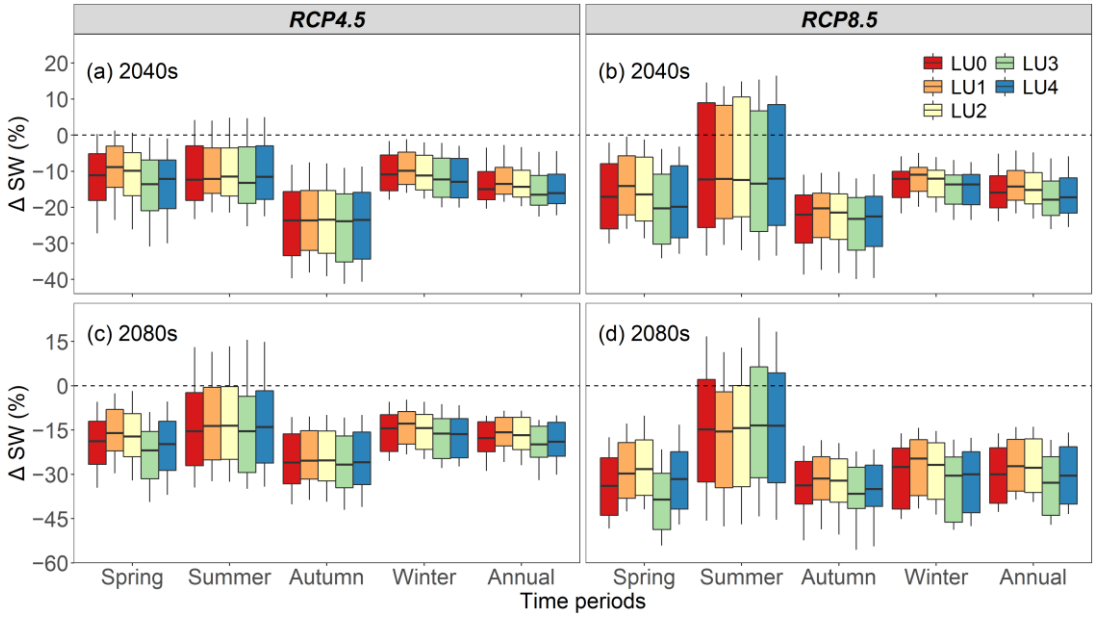

Figure 9. Projected seasonal and annual changes in soil water (%) for LU0–LU4 in the 2040s and 2080s under both RCPs estimated from 34 GCMs compared to the baseline period. Data displayed are changes in the 40−year averages for each of the 34 GCMs. The lower and upper whiskers show the 10th and 90th percentiles; box boundaries show the 25th and 75th percentiles; the black line within each box marks the median values.

3.5. Combined Effects of Climate and Land Use Changes

Under different land use change scenarios (LU1–4), projected changes in seasonal and annual runoff, ET, and SW in 2040s and 2080s compared with baseline values under both RCPs from the 34 GCMs are shown in Figures 7–9. According to the ensemble median of the 34 GCMs, the results of the four land use change scenarios (LU1–4) were only slightly different from the responses to LU0 (Figures 7–9). For instance, the ensemble median under LU2 (23.8% increase in URBN from FRST) and LU4 (29.5% increase in URBN from RNGE) showed slightly smaller annual runoff decrease than other land use scenarios (Figure 7). In addition, the ensemble median under LU3 (24.4% increase in FRST from RNGE) generally suggested a marginally less annual ET decrease than other land use scenarios (Figure 8). Furthermore, the annual soil water decrease was slightly less under LU1 (25.3% increase in RNGE from FRST) and slightly larger under LU3 (24.4% increase in FRST from RNGE) than other land use scenarios, according to the ensemble median of the 34 GCMs (Figure 9).

Figures S2–S4 show the projected change in runoff, ET, and SW for each combination of the 34 GCMs under both RCPs and different land use scenarios (LU0–4), in both future time periods compared with the baseline at the annual time scale. For the same GCM in the same future period under the same RCP, nearly all five land use scenarios (LU0–LU4) agreed on the direction of the change signal (Figures S2–S4). For instance, the climate model MI4 (RCP 4.5) showed a similar negative runoff change under LU0 (−18.9%), LU1 (−17.0%), LU2 (−14.6%), LU3 (−20.4%), and LU4 (−16.1%) in 2040s (Figure S2a). However, the direction of the change signal might be different for different land use scenarios under the same GCM when runoff changes (mm) were too small. For example, the climate model CE2 (RCP8.5) showed a positive runoff change (3.3%) under LU1 in 2040s while showing a negative runoff change under LU4 (−1.4%) (Figure S2b). Moreover, the directions of the change signal for different GCMs were quite different under the same land use scenario (Figures S2–S4). For instance, for the same land use (e.g., LU0), 9 GCMs showed a trend of increases for future runoff, with the largest increase of 41.3% (CE2), while 25 GCMs showed decreasing values, with the largest decrease of −57.7% (GF2), in 2040s under RCP 4.5 (Figure S2a). In addition, for the same future period (e.g., 2040s), generally more GCMs showed decreasing values for runoff, ET, and SW under RCP 8.5 than that under RCP 4.5 (Figures S2–S4). Furthermore, almost all GCMs showed decreasing soil water values in the future under both RCPs, and LU3 (24.4% increase in FRST from RNGE) decreased more than other land use scenarios (Figure S4).

To quantify the contribution of GCM, RCP, and LU to the uncertainty in future changes in the water balance, the ANOVA method was used and the results are presented in Figure 10. The ANOVA shows that GCMs have the greatest contribution to uncertainty, followed by RCPs, and the land use scenarios have the least contribution to future changes in runoff, ET, and SW. For instance, ANOVA (Figure 10) shows a 48.5% influence of the GCM, followed by RCP (30.4%), whereas LU had a negligible impact of 1.08% on changes in runoff.

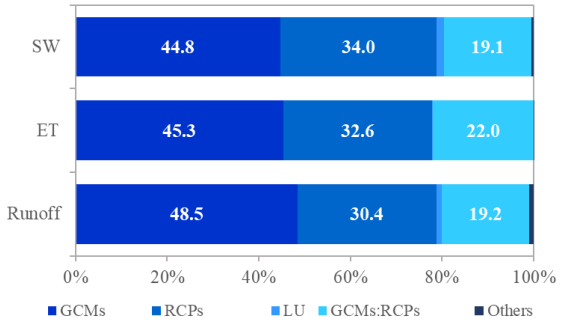

Figure 10. The contribution of uncertainty sources to the percentage change in annual runoff, ET, and SW using the three-way ANOVA.

4. Discussion

4.1. SWAT Modeling Assessment

CN2 was ranked as the most sensitive calibration parameter, implying that the generation of surface runoff is important for streamflow [77] in the Wooroloo Brook catchment. This parameter is traditionally one of the most important parameters in the SWAT model [78–81]. For instance, Saha, Zeleke [65] studied streamflow modeling using SWAT in southeastern Australia and also found that CN2 was the most sensitive parameter at daily and monthly time scales. Based on the model evaluation performance ratings proposed by earlier research [82,83], a streamflow simulation is considered acceptable when $|PBIAS| \leq 25\%$, $NSE > 0.5$, and $R^2 > 0.5$. Consequently, SWAT was judged to perform well in this catchment with $|PBIAS| \leq 8.3\%$, $NSE \geq 0.86$, and $R^2 \geq 0.87$ compared to other studies [84]. While SWAT was able to reproduce observed streamflow, there might be some difficulties in replicating peak flows (Figure S1). Earlier research [85,86] has also concluded that SWAT provided better results for low or average flows than for peak flows. A possible reason is that the routing techniques used in SWAT are sometimes inappropriate [87]. For instance, the curve number approach in the SWAT model uses mean daily rainfall without considering the intensity and duration of the rainfall [86], which may lead to difficulties in reproducing peak flows. Nevertheless, SWAT was judged to simulate the observed runoff very satisfactorily, with NSE and R^2 well above the satisfactory criteria, and the calibrated SWAT could be further applied to assess the hydrologic response to climate and land use change in this catchment.

4.2. Modeled Hydrologic Response to Land Use Change Scenarios

The clear seasonal distributions in runoff, ET, and soil water, with values greatest in winter and least in summer (Figure 5), were consistent with the seasonal variation in rainfall, which was also greatest in winter (383.9 mm) and least in summer (43.6 mm). the reason for this is that rainfall is the major element influencing runoff, ET, and SW [88], and this study catchment is a winter rainfall dominant area [89]. In addition, changes in runoff under different land use change scenarios varied across seasons, with the most notable changes appearing in winter (wet season). The seasonal runoff response to land use changes with the largest absolute changes (mm) happened in the rainy season and the smallest absolute changes (mm) in the dry period were in line with findings in other research [90,91]. However, it is noted that although the absolute change (mm) in runoff in the dry season (summer) was much smaller compared with the wet season (winter), the percentage changes (%) in runoff were noticeable during all seasons. Results indicated that mean annual actual evapotranspiration would decrease under deforestation or urbanization while increasing under afforestation, and these responses are in general agreement with the research literature [92,93]. In contrast, annual runoff increased under deforestation or urbanization while it declined under afforestation. Previous hydrologic simulations also found similar results for runoff responses to such land use changes. For instance, it was reported that the impact of clearing forest in an Australian catchment from 83 to 38% was to increase the runoff by approximately 40% [16]. This is due to the higher evapotranspiration [94] and water consumption (deep root system extracting water from shallow aquifer storage) [95] in forests, which leads to a reduction in runoff. Furthermore, mean annual soil water decreased under afforestation while it increased under deforestation using SWAT. Previous studies have found that both shallow and deep soils became very dry following tree planting [96]. Consequently, afforestation efforts in the future should consider growing tree types with low water consumption to help sustainable conservation of soil, without compromising water needs, in dry areas.

4.3. Modeled Hydrologic Response to Future Climate Change

The ensemble median of GCMs indicated that the annual maximum temperature and minimum temperature would rise by 1.0–1.3 °C in 2040s and 1.6–3.4 °C in 2080s,

regardless of emission scenarios. The temperature changes projected in this study are generally within the ranges given in previous research literature. For instance, climate projections for Southern and South-Western Flatlands showed that temperature would increase by 0.5–1.1 °C (10th to 90th percentile) by 2030 with only minor difference between the scenarios, and by 1.2–2.0 and 2.6–4.0 °C by 2090 under RCP4.5 and RCP8.5, respectively [97]. In addition to temperature, the median values of the 34 GCMs showed that rainfall was projected to decrease in all seasons and decrease greatest in spring (season of the second largest rainfall) and winter (season of the largest rainfall), in the future. For instance, rainfall was projected to decline by −35.9% in spring and −26.9% in winter by 2061–2100, under RCP 8.5. This is in agreement with earlier research. For example, Hope, Abbs [97] reported that there was high confidence that spring, winter, and annual rainfall would decline in the Southern and South-Western Flatlands in Australia, and rainfall declines were greatest during spring and winter, at 36% and 29%, respectively, by 2090 for RCP 8.5.

The considerable decreases in annual runoff projected by the multi-GCM ensemble median were consistent with the trend of changes in previous research, despite the study area, time periods, GCMs, downscaling techniques, and modeled hydrologic regimes differing across research. For example, the median forecast of 15 GCMs for an 8% decline in rainfall across SWA by 2030 was projected to reduce runoff by 25% [25]. In addition, Hope, Abbs [97] projected that runoff in SWA would decline by about 45% (median values) under RCP 4.5 and 64% under RCP 8.5 by 2090 [98]. Moreover, annual rainfall change was amplified in annual runoff change. For instance, a 2.5% change in annual runoff for 1% change in annual rainfall can be inferred from Figures 6 and 7, which is also broadly supported by previous research [25]. Moreover, annual actual evapotranspiration was also predicted to decrease (at a smaller extent compared to runoff) by −5.1% in the 2040s (RCP4.5), −6.0% in 2040s (RCP8.5), −7.5% in the 2080s (RCP4.5), and −15.8% in 2080s (RCP8.5). It is noted that the decrease in actual evapotranspiration may be related to the decreasing rainfall, although the potential evapotranspiration increases with higher temperature. This is because the study area has a small runoff coefficient (about 0.10), which means this area is relatively dry, so rainfall and soil water can also highly affect actual evapotranspiration, in addition to temperature. Furthermore, median estimates indicate that annual soil water was also projected to decline by −15.0% in 2040s (RCP4.5), −16.0% in 2040s (RCP8.5), −17.7% in 2080s (RCP4.5), and −30.0% in 2080s (RCP8.5), with the extent of decrease less than runoff and more than actual evapotranspiration. Hope, Abbs [97] also reported a projected decrease (high confidence) in soil moisture in SWA, and with extremely low soil moisture there was likely to be an increase of up to 80% more drought months in SWA by 2070 [98].

4.4. Modeled Hydrologic Responses to Combined Effects and Uncertainties

According to the ensemble median of the 34 GCMs, the results from the four land use scenarios (LU1–4) differ only slightly from the response to LU0 (Figures 7–9). Moreover, for the same GCM in the same future period under the same RCP, almost all five land use scenarios (LU0–LU4) showed a similar direction and magnitude of changes while the directions or magnitude of changes for different GCMs were quite different under the same land use scenario (Figures S2–S4). Therefore, according to Figures 7–9 and S2–S4, GCMs were expected to have much more impacts on the changes of hydrologic variables than land use scenarios. Other studies found similar trends, where changes in runoff were primarily affected by climate change whereas the role of land use change was limited compared with climate change [99]. In addition, although land use scenarios had a much smaller effect on changes in hydrologic variables compared to GCMs and RCPs, it is noteworthy that the combined impacts of land use and climate changes could further increase or decrease the future changes of hydrologic variables. For instance, annual soil water under LU3 (24.4% increase in FRST from RNGE) tended to decrease more than other land use scenarios (Figures 9 and S4). This highlights the need for reforestation programs to be

carefully targeted to maximizing ecological benefits while also minimizing soil water losses.

Previous research has shown that the selection of GCM is the major contributor to the total uncertainty, which is consistent with our results from the ANOVA analysis. For instance, Nasonova, Gusev [100] studied the streamflow response to climate change in large-scale watersheds and found that the contribution of GCMs to the runoff projection uncertainty was almost twofold higher than that of the RCPs. Karlsson, Sonnenborg [101] projected the combined effects of land use and climate changes on hydrology and found that the selection of climate models remained dominant while the contribution of land use scenarios to the average streamflow was only 1%. Therefore, caution is recommended when selecting climate models for hydrologic impacts assessment, and an ensemble of GCMs should be used to minimize the uncertainty resulting from the selection of GCMs.

4.5. Caveats and Limitations

This research concentrates on the impacts of uncertainties caused by GCMs, RCPs, and land use scenarios. However, hydrologic model structures, model parameterization, and downscaling procedures also generate uncertainties. For instance, Chen, Brissette [102] compared six downscaling techniques to study the uncertainties in quantifying climate change impacts and their results indicated that regression-based statistical downscaling techniques had a significant contribution to the uncertainty envelope. Karlsson, Sonnenborg [101] applied three hydrologic models to study the combined effects of climate models and land use scenarios and found that the hydrologic model structure also significantly affected the impact analysis results, particularly for extreme events. However, we only used one hydrological model to simulate water resource availability, and therefore this may contribute some uncertainty because of the choice of model parameters and model structure. The use of several hydrological models with different formulations was judged to improve the confidence that the likely range of simulated responses is covered [103]. Consequently, the use of an ensemble of hydrological models, different downscaling methods, and various bias correction algorithms is recommended to provide a full range and probability of future hydrologic simulations. Moreover, the CO_2 fertilization and transpiration decreases with CO_2 were not well incorporated in the hydrological modeling, which may lead to some uncertainty in the projected future changes. In addition, although the land use change scenarios considered in this study were based on present land use conditions and potential future land use plans in this catchment, we could discuss them with the state planning department in Australia to obtain more explicit land use change plans. Moreover, a change in land use could result in feedback to the regional climate. However, the interaction between land use change and regional climate was not considered in this study. In addition, current newest GCMs from CMIP6 (Coupled Model Inter-comparison Project 6) are expected to improve and enhance climate change projections for Australia [104]. Furthermore, this study focused on the Wooroloo Brook catchment, which though selected as representative of such catchments (similar climatic and hydrologic conditions), lacks repetition at the catchment scale. Therefore, more catchments, hydrologic models, different downscaling methods, and CMIP6 models will be chosen in future research to make a comprehensive range and probability of projections on future hydrology.

5. Conclusions

This study assessed the hydrologic response to climate change and land use change, both separately and when combined, in the important Wooroloo Brook catchment, located in southwestern Australia. Results showed that the SWAT model performed well in this study area, with NSE and R^2 values far larger than 0.5. Historical simulation under land use change showed that seasonal and annual runoff increased under deforestation or urbanization while declining under afforestation. Future runoff was projected to decrease more in winter and spring but decrease less in autumn and summer. Annual ET was

predicted to decrease to a smaller extent compared to runoff, whereas annual SW was projected to decrease less than runoff and more than ET. The calibrated SWAT then was applied to study the hydrologic response to combined climate and land use changes on water balance in the 2040s and 2080s periods. The results of four land use change scenarios (LU1–4) were only slightly different from the response of zero land use (LU0), according to the ensemble median of the 34 GCMs. ANOVA showed that GCM has the greatest contribution to uncertainty, followed by RCP, and the land use scenario contributes least to future changes in runoff, ET, and SW. Although the land use scenario had limited effects on the water balance compared with GCM and RCP, the joint impacts of climate and land use changes could further increase or decrease the future changes in hydrologic variables.

Supplementary Materials: The following supporting information can be downloaded at: www.mdpi.com/article/10.3390/atmos13091428/s1, Figure S1: The simulated and observed monthly streamflow for calibration (January 1992 to December 2017, data for 2008 are missing) and validation (January 1977 to December 1991) in the Wooroloo Brook catchment, SWA; Figure S2: Projected changes in runoff (%) for 34 GCMs (RCP4.5 and RCP8.5) and LU0–4 in 2040s and 2080s compared to the baseline values at annual time scale. Data showed are changes in the 40-year average values for each of the 34 GCMs under different land use scenarios; Figure S3: Projected changes in actual evapotranspiration (%) for 34 GCMs (RCP4.5 and RCP8.5) and LU0–4 in 2040s and 2080s compared to the baseline values at annual time scale. Data showed are changes in the 40-year average values for each of the 34 GCMs under different land use scenarios; Figure S4: Projected changes in soil water (%) for 34 GCMs (RCP4.5 and RCP8.5) and LU0–4 in 2040s and 2080s compared to the baseline values at annual time scale. Data showed are changes in the 40-year average values for each of the 34 GCMs under different land use scenarios; Table S1: Land use proportions for LU0–4 in the Wooroloo Brook catchment, western Australia; Table S2: The parameters calibrated and ranked in this study for the SWAT model using SWAT-CUP in the Wooroloo Brook catchment, SWA.

Author Contributions: Conceptualization, H.Z., B.W., D.L. and L.M.L.; methodology, H.Z., B.W., D.L., L.S. and M.Z.; software, H.Z. and M.Z.; validation, H.Z.; formal analysis, H.Z., B.W., D.L. and L.M.L.; investigation, H.Z.; resources, D.L., L.S. and M.Z.; data curation, D.L.; writing—original draft preparation, H.Z.; writing—review and editing, B.W., D.L., L.M.L. and Q.Y.; visualization, H.Z. and B.W.; supervision, L.M.L., D.L. and Q.Y.; project administration, L.M.L., D.L. and Q.Y.; funding acquisition, Q.Y. All authors have read and agreed to the published version of the manuscript.

Funding: This research received no external funding.

Institutional Review Board Statement: Not applicable.

Informed Consent Statement: Not applicable.

Data Availability Statement: The data applied in this study are available from the authors.

Acknowledgments: The first author acknowledges the Chinese Scholarship Council and University of Technology Sydney for scholarships and the NSW Department of Industry for providing office facilities to conduct this work. The authors thank the modelling groups, the Program for Climate Model Diagnosis and Intercomparison (PCMDI) and the WCRP's Working Group on Coupled Modelling (WGCM) for making available the WCRP CMIP5 multi-model dataset. Support of this dataset was provided by the Office of Science, US Department of Energy.

Conflicts of Interest: The authors declare no conflict of interest.

References

1. Zeng, Z.; Wang, T.; Zhou, F.; Ciais, P.; Mao, J.; Shi, X.; Piao, S. A worldwide analysis of spatiotemporal changes in water balance-based evapotranspiration from 1982 to 2009. *J. Geophys. Res. Atmos.* **2014**, *119*, 1186–1202.
2. Joseph, J.; Ghosh, S.; Pathak, A.; Sahai, A. Hydrologic impacts of climate change: Comparisons between hydrological parameter uncertainty and climate model uncertainty. *J. Hydrol.* **2018**, *566*, 1–22.
3. Seneviratne, S.I.; Corti, T.; Davin, E.L.; Hirschi, M.; Jaeger, E.B.; Lehner, I.; Orlowsky, B.; Teuling, A.J. Investigating soil moisture–climate interactions in a changing climate: A review. *Earth-Sci. Rev.* **2010**, *99*, 125–161.
4. Milly, P.C.; Dunne, K.A.; Vecchia, A.V. Global pattern of trends in streamflow and water availability in a changing climate. *Nature* **2005**, *438*, 347–350.

5. Jones, R.N.; Chiew, F.H.; Boughton, W.C.; Zhang, L. Estimating the sensitivity of mean annual runoff to climate change using selected hydrological models. *Adv. Water Resour.* **2006**, *29*, 1419–1429..
6. Reshmidevi, T.; Kumar, D.N.; Mehrotra, R.; Sharma, A. Estimation of the climate change impact on a catchment water balance using an ensemble of GCMs. *J. Hydrol.* **2018**, *556*, 1192–1204.
7. Labat, D.; Goddéris, Y.; Probst, J.L.; Guyot, J.L. Evidence for global runoff increase related to climate warming. *Adv. Water Resour.* **2004**, *27*, 631–642.
8. Legates, D.R.; Lins, H.F.; Mccabe, G.J. Comments on "Evidence for global runoff increase related to climate warming" by Labat et al. *Adv. Water Resour.* **2005**, *28*, 1310–1315.
9. Sterling, S.M.; Ducharne, A.; Polcher, J. The impact of global land-cover change on the terrestrial water cycle. *Nat. Clim. Change* **2013**, *3*, 385.
10. IPCC. Climate Change and Land: An IPCC Special Report on climate change, desertifcation, land degradation, sustainable land management, food security, and greenhouse gas fluxes in terrestrial ecosystems. In *Intergovernmental Panel on Climate Change*; pp. 1–41.
11. Mohammady, M.; Moradi, H.R.; Zeinivand, H.; Temme, A.J.A.M.; Yazdani, M.R.; Pourghasemi, H.R. Modeling and assessing the effects of land use changes on runoff generation with the CLUE-s and WetSpa models. *Theor. Appl. Climatol.* **2018**, *133*, 459–471.
12. Li, G.; Zhang, F.; Jing, Y.; Liu, Y.; Sun, G. Response of evapotranspiration to changes in land use and land cover and climate in China during 2001–2013. *Sci. Total Environ.* **2017**, *596–597*, 256–265.
13. Liu, M.; Tian, H.; Chen, G.; Ren, W.; Zhang, C.; Liu, J. Effects of Land-Use and Land-Cover Change on Evapotranspiration and Water Yield in China During 1900–2000. *J. Am. Water Resour. Assoc.* **2008**, *44*, 1193–1207.
14. Zhang, Y.W.; Shangguan, Z.P. The change of soil water storage in three land use types after 10years on the Loess Plateau. *CATENA* **2016**, *147*, 87–95.
15. Li, Q.; Cai, T.; Yu, M.; Lu, G.; Xie, W.; Bai, X. Investigation into the impacts of land-use change on runoff generation characteristics in the upper Huaihe River Basin, China. *J. Hydrol. Eng.* **2013**, *18*, 1464–1470.
16. Siriwardena, L.; Finlayson, B.; McMahon, T. The impact of land use change on catchment hydrology in large catchments: The Comet River, Central Queensland, Australia. *J. Hydrol.* **2006**, *326*, 199–214.
17. Bruijnzeel, L.A. Hydrological Functions of Tropical Forests: Not Seeing the Soil for the Trees? *Agric. Ecosyst. Environ.* **2004**, *10401*, 185–228.
18. Sun, G.; Zhou, G.; Zhang, Z.; Wei, X.; G.McNulty, S.; Vose, J.M. Potential water yield reduction due to forestation across China. *J. Hydrol.* **2006**, *328*, 548–558.
19. Buttle, J.M.; Metcalfe, R.A. Boreal forest disturbance and streamflow response, northeastern Ontario. *Can. J. Fish. Aquat. Sci.* **2000**, *57*, 5–18.
20. Ceballos-Barbancho, A.; Morán-Tejeda, E.; Luengo-Ugidos, M.; Llorente-Pinto, J.M. Water resources and environmental change in a Mediterranean environment: The south-west sector of the Duero river basin (Spain). *J. Hydrol.* **2008**, *351*, 126–138.
21. Zhou, G.; Wei, X.; Luo, Y.; Zhang, M.; Li, Y.; Qiao, Y.; Liu, H.; Wang, C. Forest recovery and river discharge at the regional scale of Guangdong Province, China. *Water Resour. Res.* **2010**, *46*, 5109–5115.
22. Zhou, G.; Wei, X.; Chen, X.; Zhou, P.; Liu, X.; Xiao, Y.; Sun, G.; Scott, D.F.; Zhou, S.; Han, L. Global pattern for the effect of climate and land cover on water yield. *Nat. Commun.* **2015**, *6*, 5918.
23. CSIRO and Bureau of Meteorology. *Climate Change in Australia Information for Australia's Natural Resource Management Regions: Technical Report*; CSIRO and Bureau of Meteorology: Australia, 2015.
24. Heinzeller, D.; Junkermann, W.; Kunstmann, H. Anthropogenic aerosol emissions and rainfall decline in Southwestern Australia: Coincidence or causality? *J. Clim.* **2016**, *29*, 8471–8493.
25. Silberstein, R.; Aryal, S.; Durrant, J.; Pearcey, M.; Braccia, M.; Charles, S.; Boniecka, L.; Hodgson, G.; Bari, M.; Viney, N. Climate change and runoff in south-western Australia. *J. Hydrol.* **2012**, *475*, 441–455.
26. Petrone, K.C.; Hughes, J.D.; Van Niel, T.G.; Silberstein, R.P. Streamflow decline in southwestern Australia, 1950–2008. *Geophys. Res. Lett.* **2010**, *37*, L11401. https://doi.org/10.1029/2010GL043102.
27. Charles S.; Silberstein, R.; Teng, J.; Fu, G.; Hodgson, G.; Gabrovsek, C.; Crute, J.; Chiew, F.H.S.; Smith, I.N.; Kirono, D.G.C.; et al. *Climate analyses for south-west Western Australia. A report to the Australian Government from the CSIRO South-West Western Australia Sustainable Yields Project*; CSIRO: Australia, 2010; 83p.
28. Fraser, E.D.; Simelton, E.; Termansen, M.; Gosling, S.N.; South, A. "Vulnerability hotspots": Integrating socio-economic and hydrological models to identify where cereal production may decline in the future due to climate change induced drought. *Agric. For. Meteorol.* **2013**, *170*, 195–205.
29. Teng, J.; Chiew, F.; Vaze, J.; Marvanek, S.; Kirono, D. Estimation of climate change impact on mean annual runoff across continental Australia using Budyko and Fu equations and hydrological models. *J. Hydrometeorol.* **2012**, *13*, 1094–1106.
30. Mpelasoka, F.; Hennessy, K.; Jones, R.; Bates, B. Comparison of suitable drought indices for climate change impacts assessment over Australia towards resource management. *Int. J. Climatol.* **2008**, *28*, 1283–1292.
31. Callow, J.N. *River Response to Land Clearing and Landscape Salinisation in Southwestern Australia*; University of Western Australia: Perth, WA, Australia, 2007.
32. Gilfedder, M.; Walker, G.R.; Dawes, W.R.; Stenson, M.P. Prioritisation approach for estimating the biophysical impacts of land-use change on stream flow and salt export at a catchment scale. *Environ. Model. Softw.* **2009**, *24*, 262–269.

33. McFarlane, D.; Stone, R.; Martens, S.; Thomas, J.; Silberstein, R.; Ali, R.; Hodgson, G. Climate change impacts on water yields and demands in south-western Australia. *J. Hydrol.* **2012**, *475*, 488–498.
34. Barron, O.; Silberstein, R.; Ali, R.; Donohue, R.; McFarlane, D.; Davies, P.; Hodgson, G.; Smart, N.; Donn, M. Climate change effects on water-dependent ecosystems in south-western Australia. *J. Hydrol.* **2012**, *434*, 95–109.
35. Wilson, M. *Identifying Rainfall Decline and Land Use Impacts on Runoff from Catchments in Southwest Western Australia*; University of Western Australia: Perth, WA, Australia, 2012.
36. Chen, J.; Brissette, F.P.; Poulin, A.; Leconte, R. Overall uncertainty study of the hydrological impacts of climate change for a Canadian watershed. *Water Resour. Res.* **2011**, *47*, W12509.
37. Crosbie, R.S.; McCallum, J.L.; Walker, G.R.; Chiew, F.H. Modelling climate-change impacts on groundwater recharge in the Murray-Darling Basin, Australia. *Hydrogeol. J.* **2010**, *18*, 1639–1656.
38. Shen, M.; Chen, J.; Zhuan, M.; Chen, H.; Xu, C.-Y.; Xiong, L. Estimating uncertainty and its temporal variation related to global climate models in quantifying climate change impacts on hydrology. *J. Hydrol.* **2018**, *556*, 10–24.
39. Zhang, H.; Huang, G.H. Development of climate change projections for small watersheds using multi-model ensemble simulation and stochastic weather generation. *Clim. Dyn.* **2013**, *40*, 805–821.
40. Notebaert, B.; Verstraeten, G.; Ward, P.; Renssen, H.; Van Rompaey, A. Modeling the sensitivity of sediment and water runoff dynamics to Holocene climate and land use changes at the catchment scale. *Geomorphology* **2011**, *126*, 18–31.
41. Anache, J.A.; Flanagan, D.C.; Srivastava, A.; Wendland, E.C. Land use and climate change impacts on runoff and soil erosion at the hillslope scale in the Brazilian Cerrado. *Sci. Total Environ.* **2018**, *622*, 140–151.
42. Liu, J.; Zhang, C.; Kou, L.; Zhou, Q. Effects of climate and land use changes on water resources in the Taoer river. *Adv. Meteorol.* **2017**, *2017*, 1031854.
43. Arnold, J.G.; Srinivasan, R.; Muttiah, R.S.; Williams, J.R. Large area hydrologic modeling and assessment part I: Model development. *J. Am. Water Resour. Assoc.* **1998**, *34*, 73–89.
44. Wang, S.; Kang, S.; Zhang, L.; Li, F. Modelling hydrological response to different land-use and climate change scenarios in the Zamu River basin of northwest China. *Hydrol. Processes Int. J.* **2008**, *22*, 2502–2510.
45. Arnold, J.G.; Fohrer, N. SWAT2000: Current capabilities and research opportunities in applied watershed modelling. *Hydrol. Processes Int. J.* **2005**, *19*, 563–572.
46. Wu, F.; Zhan, J.; Su, H.; Yan, H.; Ma, E. Scenario-based impact assessment of land use/cover and climate changes on watershed hydrology in Heihe River Basin of northwest China. *Adv. Meteorol.* **2015**, *2015*, 410198.
47. Park, J.-Y.; Park, M.-J.; Joh, H.-K.; Shin, H.-J.; Kwon, H.-J.; Srinivasan, R.; Kim, S.-J. Assessment of MIROC3. 2 HiRes climate and CLUE-s land use change impacts on watershed hydrology using SWAT. *Trans. ASABE* **2011**, *54*, 1713–1724.
48. Gabiri, G.; Diekkrüger, B.; Näschen, K.; Leemhuis, C.; Linden, R.v.d.; Majaliwa, J.-G.M.; Obando, J.A. Impact of Climate and Land Use/Land Cover Change on the Water Resources of a Tropical Inland Valley Catchment in Uganda, East Africa. *Climate* **2020**, *8*, 83.
49. Shrestha, M.K.; Recknagel, F.; Frizenschaf, J.; Meyer, W. Future climate and land uses effects on flow and nutrient loads of a Mediterranean catchment in South Australia. *Sci. Total Environ.* **2017**, *590*, 186–193.
50. Degens, B.; Muirden, P.; Kelly, B.; Allen, M. Acidification of salinised waterways by saline groundwater discharge in south-western Australia. *J. Hydrol.* **2012**, *470*, 111–123.
51. Viney, N.R.; Sivapalan, M. A conceptual model of sediment transport: Application to the Avon River Basin in Western Australia. *Hydrol. Processes Int. J.* **1999**, *13*, 727–743.
52. Mulligan, D.R. *Environmental Management in the Australian Minerals and Energy Industries: Principles and Practices*; UNSW Press: 1996.
53. Garnett, S.; Szabo, J.; Dutson, G. *The Action Plan for Australian Birds 2010*; CSIRO Publishing: 2011.
54. CSIRO. *Surface Water Yields in South-West Western Australia. A Report to the Australian Government from the CSIRO South-West Western Australia Sustainable Yields Project*; CSIRO Water for a Healthy Country Flagship: Australia, 2009.
55. Gassman, P.W.; Reyes, M.R.; Green, C.H.; Arnold, J.G. The soil and water assessment tool: Historical development, applications, and future research directions. *Trans. ASABE* **2007**, *50*, 1211–1250.
56. Bondelid, T.R.; McCuen, R.H.; Jackson, T.J. Sensitivity of SCS Models to Curve Number Variation 1. *J. Am. Water Resour. Assoc.* **1982**, *18*, 111–116.
57. Baker, T.J.; Miller, S.N. Using the Soil and Water Assessment Tool (SWAT) to assess land use impact on water resources in an East African watershed. *J. Hydrol.* **2013**, *486*, 100–111.
58. Zhang, A.; Zhang, C.; Fu, G.; Wang, B.; Bao, Z.; Zheng, H. Assessments of impacts of climate change and human activities on runoff with SWAT for the Huifa River Basin, Northeast China. *Water Resour. Manag.* **2012**, *26*, 2199–2217.
59. Narsimlu, B.; Gosain, A.K.; Chahar, B.R. Assessment of future climate change impacts on water resources of Upper Sind River Basin, India using SWAT model. *Water Resour. Manag.* **2013**, *27*, 3647–3662.
60. Saha, P.P.; Zeleke, K. Rainfall-Runoff modelling for sustainable water resources management: SWAT model review in Australia. In *Sustainability of Integrated Water Resources Management*; Springer: Berlin/Heidelberg, Germany, 2015; pp. 563–578.
61. Brown, S.C.; Versace, V.L.; Lester, R.E.; Walter, M.T. Assessing the impact of drought and forestry on streamflows in south-eastern Australia using a physically based hydrological model. *Environ. Earth Sci.* **2015**, *74*, 6047–6063.
62. Liu, D.L.; Zuo, H. Statistical downscaling of daily climate variables for climate change impact assessment over New South Wales, Australia. *Clim. Change* **2012**, *115*, 629–666.

63. Roti, V.; Kashyap, P.; Anilkumar, S.R.; Srivastava, R.; Harish, C. Runoff and sediment yield estimation by SWAT model: Review and outlook. *Int. J. Curr. Microbiol. Appl. Sci.* **2018**, *7*, 879–886.
64. Zhang, X.; Xu, Y.-P.; Fu, G. Uncertainties in SWAT extreme flow simulation under climate change. *J. Hydrol.* **2014**, *515*, 205–222.
65. Saha, P.P.; Zeleke, K.; Hafeez, M. Streamflow modeling in a fluctuant climate using SWAT: Yass River catchment in south eastern Australia. *Environ. Earth Sci.* **2014**, *71*, 5241–5254.
66. McKenzie, N.; Jacquier, D.; Ashton, L.; Cresswell, H. Estimation of soil properties using the Atlas of Australian Soils. *CSIRO Land Water Tech. Rep.* **2000**, *11*, 1–12.
67. Sirisena, T.; Maskey, S.; Ranasinghe, R.; Babel, M.S. Effects of different precipitation inputs on streamflow simulation in the Irrawaddy River Basin, Myanmar. *J. Hydrol.* **2018**, *19*, 265–278.
68. Ghaffari, G.; Keesstra, S.; Ghodousi, J.; Ahmadi, H. SWAT-simulated hydrological impact of land-use change in the Zanjanrood basin, Northwest Iran. *Hydrol. Processes Int. J.* **2010**, *24*, 892–903.
69. Abbaspour, K.C. *SWAT-CUP 2012: SWAT Calibration and Uncertainty Programs–A User Manual*; Eawag: Dübendorf, Switzerland, 2013; Volume 103.
70. Abbaspour, K.C.; Yang, J.; Maximov, I.; Siber, R.; Bogner, K.; Mieleitner, J.; Zobrist, J.; Srinivasan, R. Modelling hydrology and water quality in the pre-alpine/alpine Thur watershed using SWAT. *J. Hydrol.* **2007**, *333*, 413–430.
71. Nash, J.E.; Sutcliffe, J.V. River flow forecasting through conceptual models part I—A discussion of principles. *J. Hydrol.* **1970**, *10*, 282–290.
72. Shi, P.; Chen, C.; Srinivasan, R.; Zhang, X.; Cai, T.; Fang, X.; Qu, S.; Chen, X.; Li, Q. Evaluating the SWAT model for hydrological modeling in the Xixian watershed and a comparison with the XAJ model. *Water Resour. Manag.* **2011**, *25*, 2595–2612.
73. Wang, B.; Deveson, E.D.; Waters, C.; Spessa, A.; Lawton, D.; Feng, P.; Li Liu, D. Future climate change likely to reduce the Australian plague locust (Chortoicetes terminifera) seasonal outbreaks. *Sci. Total Environ.* **2019**, *668*, 947–957.
74. Moriasi, D.N.; Pai, N.; Steiner, J.L.; Gowda, P.H.; Winchell, M.; Rathjens, H.; Starks, P.J.; Verser, J.A. SWAT-LUT: A Desktop Graphical User Interface for Updating Land Use in SWAT. *J. Am. Water Resour. Assoc.* **2019**, *55*, 1102–1115. https://doi.org/10.1111/1752-1688.12789.
75. Aryal, A.; Shrestha, S.; Babel, M.S. Quantifying the sources of uncertainty in an ensemble of hydrological climate-impact projections. *Theor. Appl. Climatol.* **2019**, *135*, 193–209.
76. Shi, L.; Feng, P.; Wang, B.; Li Liu, D.; Cleverly, J.; Fang, Q.; Yu, Q. Projecting potential evapotranspiration change and quantifying its uncertainty under future climate scenarios: A case study in southeastern Australia. *J. Hydrol.* **2020**, *584*, 124756.
77. Guo, J.; Su, X. Parameter sensitivity analysis of SWAT model for streamflow simulation with multisource precipitation datasets. *Hydrol. Res.* **2019**, *50*, 861–877.
78. Abbas, N.; Wasimi, S.A.; Bhattarai, S.; Al-Ansari, N. The Impacts of Climate Change on Fitzroy River Basin, Queensland, Australia: The Impacts of Climate Change on Fitzroy River Basin, Queensland, Australia. *J. Civ. Eng. Archit.* **2017**, *11*, 38–47.
79. Feyereisen, G.; Strickland, T.; Bosch, D.; Sullivan, D. Evaluation of SWAT manual calibration and input parameter sensitivity in the Little River watershed. *Trans. ASABE* **2007**, *50*, 843–855.
80. Das, B.; Jain, S.; Singh, S.; Thakur, P. Evaluation of multisite performance of SWAT model in the Gomti River Basin, India. *Appl. Water Sci.* **2019**, *9*, 134.
81. Nossent, J.; Elsen, P.; Bauwens, W. Sobol'sensitivity analysis of a complex environmental model. *Environ. Model. Softw.* **2011**, *26*, 1515–1525.
82. Wallace, C.W.; Flanagan, D.C.; Engel, B.A. Evaluating the effects of watershed size on SWAT calibration. *Water* **2018**, *10*, 898.
83. Moriasi, D.N.; Arnold, J.G.; Van Liew, M.W.; Bingner, R.L.; Harmel, R.D.; Veith, T.L. Model evaluation guidelines for systematic quantification of accuracy in watershed simulations. *Trans. ASABE* **2007**, *50*, 885–900.
84. Lee, S.; Yeo, I.Y.; Sadeghi, A.M.; Mccarty, G.W.; Hively, W.D.; Lang, M.W.; Sharifi, A. *Comparative Analyses of Hydrological Responses of Two Adjacent Watersheds to Climate Variability and Change Using the SWAT Model*; Copernicus GmbH: 2017.
85. Fukunaga, D.C.; Cecílio, R.A.; Zanetti, S.S.; Oliveira, L.T.; Caiado, M.A.C. Application of the SWAT hydrologic model to a tropical watershed at Brazil. *CATENA* **2015**, *125*, 206–213.
86. Shrestha, M.K.; Recknagel, F.; Frizenschaf, J.; Meyer, W. Assessing SWAT models based on single and multi-site calibration for the simulation of flow and nutrient loads in the semi-arid Onkaparinga catchment in South Australia. *Agric. Water Manag.* **2016**, *175*, 61–71.
87. Kim, N.W.; Lee, J. Enhancement of the channel routing module in SWAT. *Hydrol. Processes Int. J.* **2010**, *24*, 96–107.
88. Fekete, B.M.; Vörösmarty, C.J.; Roads, J.O.; Willmott, C.J. Uncertainties in Precipitation and Their Impacts on Runoff Estimates. *J. Clim.* **2004**, *17*, 294–304.
89. Chiew, F.H.; McMahon, T.A. Modelling the impacts of climate change on Australian streamflow. *Hydrol. Processes Int. J.* **2002**, *16*, 1235–1245.
90. Brown, A.E.; Zhang, L.; McMahon, T.A.; Western, A.W.; Vertessy, R.A. A review of paired catchment studies for determining changes in water yield resulting from alterations in vegetation. *J. Hydrol.* **2005**, *310*, 28–61.
91. Zhang, H.; Wang, B.; Li Liu, D.; Zhang, M.; Leslie, L.M.; Yu, Q. Using an improved SWAT model to simulate hydrological responses to land use change: A case study of a catchment in tropical Australia. *J. Hydrol.* **2020**, *585*, 124822.
92. Lin, B.; Chen, X.; Yao, H.; Chen, Y.; Liu, M.; Gao, L.; James, A. Analyses of landuse change impacts on catchment runoff using different time indicators based on SWAT model. *Ecol. Indic.* **2015**, *58*, 55–63.

93. Wattenbach, M.; Zebisch, M.; Hattermann, F.; Gottschalk, P.; Goemann, H.; Kreins, P.; Badeck, F.; Lasch, P.; Suckow, F.; Wechsung, F. Hydrological impact assessment of afforestation and change in tree-species composition–a regional case study for the Federal State of Brandenburg (Germany). *J. Hydrol.* **2007**, *346*, 1–17.
94. Hundecha, Y.; Bárdossy, A. Modeling of the effect of land use changes on the runoff generation of a river basin through parameter regionalization of a watershed model. *J. Hydrol.* **2004**, *292*, 281–295.
95. Mwangi, H.M.; Julich, S.; Patil, S.D.; McDonald, M.A.; Feger, K.H. Modelling the impact of agroforestry on hydrology of Mara River Basin in East Africa. *Hydrol. Processes Int. J.* **2016**, *30*, 3139–3155.
96. Jia, X.; Zhu, Y.; Luo, Y. Soil moisture decline due to afforestation across the Loess Plateau, China. *J. Hydrol.* **2017**, *546*, 113–122.
97. Hope, P.; Abbs, D.; Bhend, J.; Chiew, F.; Church, J.; Ekström, M.; Kirono, D.; Lenton, A.; Lucas, C.; McInnes, K. Southern and South-Western Flatlands cluster report, climate change in Australia: Projections for Australia's natural resource management regions. In *Cluster Reports*; CSIRO and Bureau of Meteorology: Australia, 2015.
98. Sudmeyer, R.; Edward, A.; Fazakerley, V.; Simpkin, L.; Foster, I. *Climate Change: Impacts and Adaptation for Agriculture in Western Australia*; Bulletin 4870; Department of Agriculture and Food: Perth, WA, Australia, 2016.
99. Phung, Q.A.; Thompson, A.L.; Baffaut, C.; Costello, C.; Sadler, E.J.; Svoma, B.M.; Lupo, A.; Gautam, S. Climate and Land Use Effects on Hydrologic Processes in a Primarily Rain-Fed, Agricultural Watershed. *J. Am. Water Resour. Assoc.* **2019**, *55*, 1196–1215.
100. Nasonova, O.N.; Gusev, Y.M.; Kovalev, E.E.; Ayzel, G.V. Climate change impact on streamflow in large-scale river basins: Projections and their uncertainties sourced from GCMs and RCP scenarios. *Proc. Int. Assoc. Hydrol. Sci.* **2018**, *379*, 139.
101. Karlsson, I.B.; Sonnenborg, T.O.; Refsgaard, J.C.; Trolle, D.; Børgesen, C.D.; Olesen, J.E.; Jeppesen, E.; Jensen, K.H. Combined effects of climate models, hydrological model structures and land use scenarios on hydrological impacts of climate change. *J. Hydrol.* **2016**, *535*, 301–317.
102. Chen, J.; Brissette, F.P.; Leconte, R. Uncertainty of downscaling method in quantifying the impact of climate change on hydrology. *J. Hydrol.* **2011**, *401*, 190–202.
103. CSIRO. *Description of Project Methods. South-West Western Australia Sustainable Yields Project*; CSIRO: Australia, 2010; 83p.
104. Grose, M.R.; Narsey, S.; Delage, F.; Dowdy, A.J.; Bador, M.; Boschat, G.; Chung, C.; Kajtar, J.; Rauniyar, S.; Freund, M. Insights from CMIP6 for Australia's future climate. *Earth's Future* **2020**, *8*, e2019EF001469.